TELKOMNIKA, Vol.13, No.3, September 2015, pp. 828~835
ISSN: 1693-6930, accredited A by DIKTI, Decree No: 58/DIKTI/Kep/2013
DOI: 10.12928/TELKOMNIKA.v13i3.2092

Online Correction of the Dynamic Errors in a Stored Overpressure Measurement System

Wei Wang[1]*, Zhijie Zhang[2]
School of Instrument and Electronics, North University of China, Taiyuan, China
*Corresponding author, e-mail: 2002ww2002@126.com

Abstract

The problem encountered in sharp shock testing as a result of inadequate bandwidth must be addressed to obtain an accurate overpressure peak value when measuring the steep signals of shockwaves during explosions. A dynamic compensator can effectively amend the dynamic errors caused by sensor system characteristics; thus, a dynamic compensation method based on improved particle swarm optimization (PSO) algorithm is proposed in this paper. This method can effectively overcome the influence of the initial value derived with PSO algorithm on compensator index. The distributed algorithm is introduced into the hardware structure design of the dynamic compensator to facilitate the application of an optimized compensator to real-time online measurement. This integration realizes the high-speed parallel of the dynamic compensator of the sensor with field-programmable gate array. Experimental results show that a high-speed parallel dynamic compensator can amend the dynamic errors in a sensor accurately and in a timely manner.

Keywords: *dynamic compensation method, improved particle swarm optimized algorithm, distributed algorithm, FPGA*

1. Introduction

A dynamic testing system is installed underground to test explosion shockwaves. A sensor interface is located above ground. The spectrum of the pressure sensor cannot cover the signal spectrum under the influence of the cliff front of the shockwave. Thus, signal amplitude increases significantly. The areas selected by the dynamic testing system are shocked sharply, and peak overpressure cannot be determined accurately when the sensor approaches resonant frequency. Hence, the amplitude frequency characteristics of a piezoelectric sensor should be compensated. Compensation methods include inverse filtering, the collocation of zero poles, and system identification [1]. In addition, neural network, particle swarm optimization (PSO) algorithm, and other algorithms are adopted to improve compensation precision.

Neural networks can easily be trapped in the local minimum regardless of network search speed, and Internet precision is difficult to improve at latter stages of training. Although the PSO algorithm is a holistic optimal algorithm, the initial position of the particle affects the optimization results of this algorithm [2]. On the basis of the aforementioned principles, the present paper proposes an improved PSO algorithm that employs adaptive neural networks to determine the optimal initial value for each particle in the particle swarm within the shortest time. This algorithm eventually yields a holistic optimal value.

The dynamic compensator is normally of high order, and the dynamic errors of the sensor are difficult to amend quickly and in real time according to the programming ideas of the traditional displacement summation [3]. The current study establishes a parallel method to develop hardware for dynamic compensation filtering according to the concepts of the distributed algorithm. This method converts the index of optimal dynamic compensation filtering as obtained with the improved PSO algorithm into the ROM look-up table operation while avoiding the multiplication operation. Compensation results can be generated through the performance of a simple data addition operation after the look-up table is introduced. This process significantly increases operation speed. Finally, this method can effectively measure dynamic compensators in real time.

Received March 12, 2015; Revised June 2, 2015; Accepted June 20, 2015

2. Amendment Method of Sensor Dynamic Errors Based on PSO Algorithm

Figure 1 shows the general principles of dynamic errors in sensors based on the improved PSO algorithm. $y(k)$ is the sensor output, $r(k)$ is the output of the reference model, $z(k)$ is the compensated output, and m is the compensator order.

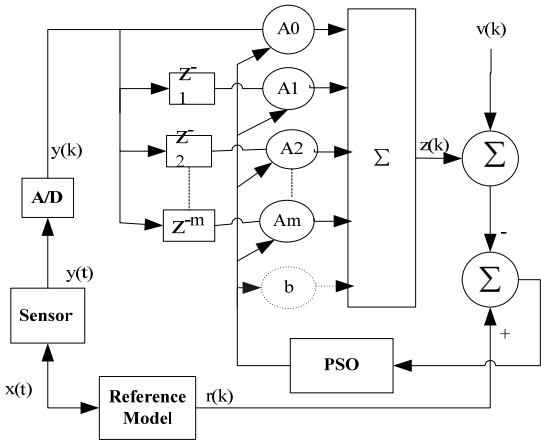

Figure 1. Schematic of sensor dynamic errors

According to the input vector of the algorithm, $X(k)$ can be expressed as follows:

$$X(k) = [y(k), y(k-1) \cdots y(k-m)] \tag{1}$$

Compensator index is determined as follows:

$$W = [A_0, A_1 \cdots A_{m-1}, A_m]^T \tag{2}$$

The compensated output from Formulas (1) and (2) is obtained using:

$$z(k) = W \cdot X(k) + v(k) \tag{3}$$

Where $v(k)$ is the uncorrelated random noise that follows the normal distribution. The mean squared errors between $z(k)$ and $r(k)$ are determined using:

$$J = \frac{1}{N} \times \sum_{k=0}^{N} [r(k) - z(k)]^2 \tag{4}$$

Adaptive neutral networks determine the optimal initial value for the PSO algorithm according to Formula (5) for continual renewal.

$$z(k) = W(k-1) \cdot X(k) + b(k-1) \tag{5}$$

Where $W(k-1)$ and $b(k-1)$ represent the compensated index and threshold, respectively, when the compensated network trains to the $k-1$th step.

The compensated index and threshold are renewed according to Formulas (6) and (7) during the neural network training process.

$$W(k+1) = W(k) + \alpha \times X(k+1) \times e(k) \tag{6}$$

$$b(k+1) = b(k) + \alpha \times e(k+1) \quad (7)$$

Where α is the study factor whose parameters should not be excessively large to meet convergence requirements. This variable typically takes a value of 0 < α < 1.

We regard Formula (4) as the standard in the entire process of adaptive neutral network training. The dynamic compensator index obtained is the initial value of the PSO algorithm when training reaches a stage in which the mean squared errors and J are less than a set value or when the training times reach a certain value [4].

When we apply the PSO algorithm to solve dynamic compensator index, we should encode the algorithm properly to generate the particle. On the basis of PSO algorithm characteristics, a real number can be used to represent each parameter. In addition, if W represents the current location of each particle, then another particle that corresponds to v should be generated to represent particle speed. Fitness function $F(W)$ assesses the pros and cons of the current location [5]. Among these variables, W is an m-dimensional variable; therefore, v should be an m-dimensional variable as well so that the particle can adopt the following code structure:

$A_0, A_1 \cdots A_{m-1}, A_m$	$v_0, v_1, v_2 \cdots v_{m-2}, v_{m-1}, v_m$	$F(W)$

Figure 2. Code structure diagram of the particle in the PSO algorithm

The PSO algorithm uses the adaptive function to determine the pros and cons of the current particle location. Once the algorithm is completed, the optimum solution obtained is the smallest particle throughout the operation. This value represents the parameter value. Finally, compensator index is derived [6].

3. Algorithm Verification

Given this hardware design, the pressure sensor is primarily studied through dynamic calibration experiments and computer simulations. Then, the PSO algorithm is applied for optimization according to the input and output data of the sensor and of the reference model. Specifically, the algorithm is verified through a dynamic calibration experiment that emphasizes the pressure sensor. In this experiment, the shock tube shown in Figure 3 generates a step pressure as a standard signal that is incorporated into the measured pressure sensor by analyzing the response of the pressure sensor output, calibrating this sensor, and studying the actual working performance. The curve depicted in Figure 4 is the actual measured response curve of the specific pressure sensor.

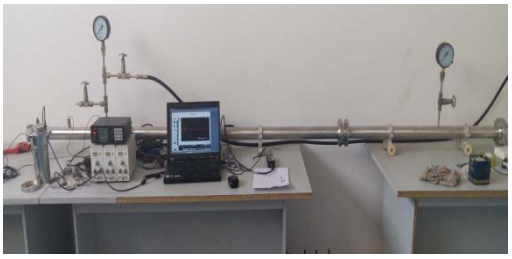

Figure 3. Shock tube

The improved PSO algorithm can be used in the inverse modeling of the sensor. Then, the sensor output can be equated to compensated system input. Thus, the curve can be regarded as compensated system input and the reference model as the ideal step signal.

Furthermore, indices a and b of the sensor dynamic compensated filter are obtained, where a = [1.1223, −0.2144, −0.3357, 0.3262] and b = [1.2817, −1.0131, 0.2533, 0.5381].

The compensation result is illustrated as curve 2, where the response time after compensation is 10 μs, the overshoot is 10%, and all results meet the technical indicator requirements. The simulation results obtained in MATLAB show that response is accelerated and that the working frequency band broadens. Moreover, noise is effectively removed.

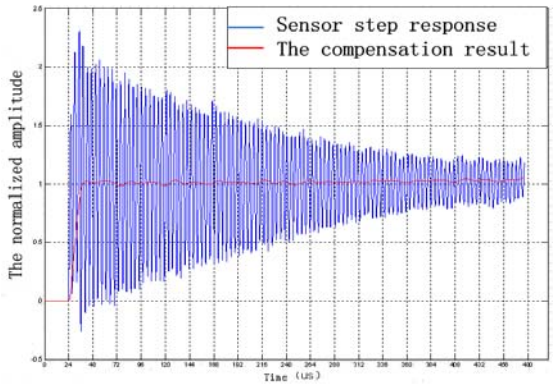

Figure 4. Compensated results for the sensor

4. System Hardware Design

Digital signal processor devices are incompetent for the system when a dynamic compensated filter is used in real-time cases with high requirements.

Nonetheless, field-programmable gate array (FPGA) devices serve as excellent carriers for this filter given the look-up table structure and parallel processing capability of such devices [7]. This study designs a data storage system in which FPGA is the core control unit. This system includes components such as power management, AD control, data storage, and data transmission modules. The hardware circuit structure designed in this study is depicted in Figure 5.

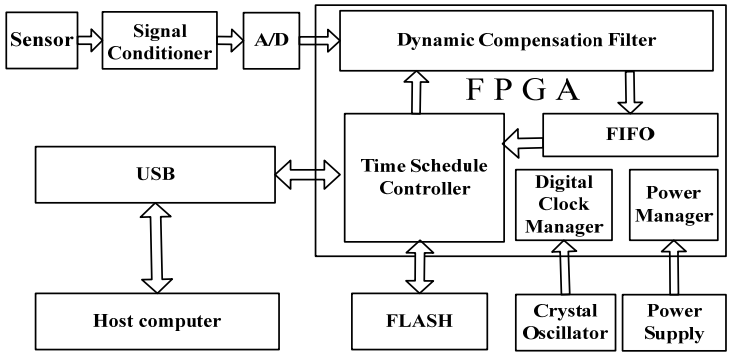

Figure 5.Hardware circuit structure

4.1. Pressure Sensor

Charge amplifiers have been incorporated into piezoelectric pressure sensors because of the recent development in integrated circuit technology. Such sensors are known as integrated circuit piezoelectric (ICP) pressure sensors. Such sensors can overcome the disadvantage of traditional pressure sensors and exhibit a strong anti-interference capability due to the presence of the internal charge amplifier [8]. ICP pressure sensors have significantly improved test accuracy and reliability in comparison with traditional pressure sensors. Thus, ICP

pressure sensors are an ideal choice as shockwave pressure sensors. This study uses the ICP pressure sensor from the 113 series manufactured by The PCB Company. The range of this sensor is from 50 psi to 1000 psi. In designing the conditioning circuit of the following signals to ensure stability, the resonant frequency of the sensor is over 500 kHz, the response time is shorter than 1 μs, non-linear is lower than 1% FS, and output impedance is less than 100 Ω.

4.2. Signal Conditioning Circuit

Signal conditioning circuits convert the output signal of the sensor to meet the requirements of the subsequent acquisition circuit. The transformation relation is illustrated in Figure 6. The full output signal range of the ICP pressure sensor is 5 V, the offset voltage ranges from 8 V to 14 V, and the sample voltage of the subsequent acquisition circuit ranges from 0 V to 2.5 V. Therefore, the first step in deriving the conditioning signal involves exchanging the coupling signal and then entering the scaling circuit. The design above is premised on the condition of full sensor range. In practice, small signal testing situations are observed. Therefore, we should amplify the effective output signal of the sensor to fully utilize the number of significant A/D converter digits for improving testing accuracy.

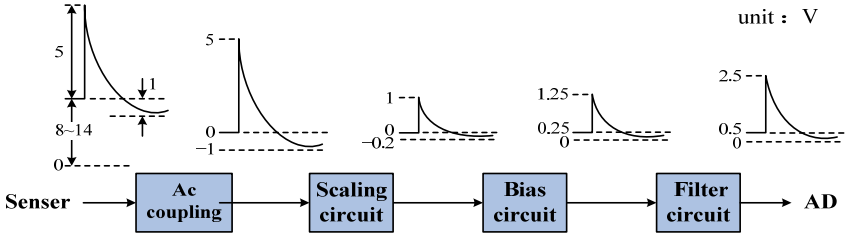

Figure 6. Signal conditioning circuit and signal transform relation

4.3. Sampling Storage Circuit

Sampling storage circuits quantify the sampling process and store shockwave signal records. This circuit consists of an A/D converter and memory, as depicted in Figure 7. This study obtained the approximation A/D converter AD7482 from the Analog Devices Company. The resolution of this converter is 12 bits and can reach 3 MHz. Four types of programmable sampling frequencies are detected in this scenario: 2, 1, 500, and 250 kHz. To accelerate data access, the system utilizes static random access memory with a storage capacity of 2 MW. Four types of programmable system record capacities are considered as well:2, 1, 512, and 256 kW.

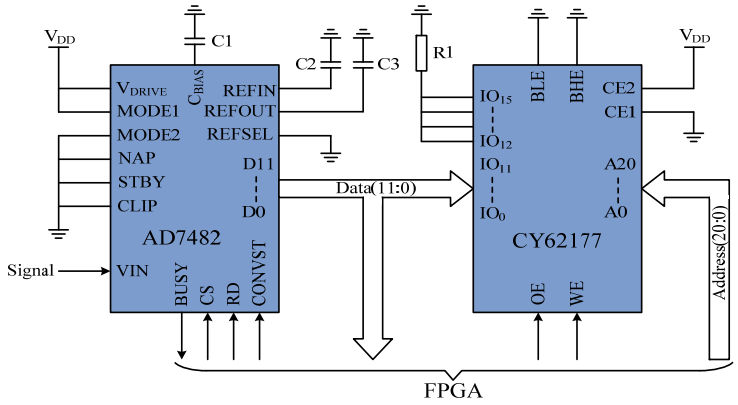

Figure 7. Block diagram of the sampling storage circuit

4.4. Dynamic Compensated Filter Based on FPGA

To produce the dynamic compensator in FPGA, we must divide this array into six submodulars: AD control, data control, shift register, look-up table, cumulative sum, and data storage modules.

a) The AD control module mainly ensures the precise sampling of AD7482 under a preset sampling rate, as well as the timely output of the AD conversion result from AD7482 data.
b) The data control module primarily facilitates the cooperation of AD with other modules in latching the AD7482 conversion result within the FPGA to perform other functions [9].
c) The shift register mainly shifts the data of each register according to the order of the compensated filter. This register then stores the AD results in the lowest part of each register [10].
d) The look-up table module mainly stores all probable typing calculation results for the computation of the dynamic compensated filter index and to look up the precise calculation result input at that moment according to the typing and result outputs [11].
e) The cumulative sum module primarily shifts the summation of the output data in the look-up table to perform the multiplication function through addition.
f) The data storage module mainly stores the compensated results in FLASH according to the time sequence presented in the FLASH chip handbook.

4.5. USB Drive

The storage record module displays a USB interface. The circuit of this module is established with the aid of a USB drive and is controlled by microcontrollers. This study uses the FT245R USB drive produced by Future Technology Devices International. The transmission rate of this drive can reach 8 Mbps. Moreover, the drive has a 256 B receive buffer and a 128 B send buffer. This USB drive can supply power through a USB bus or through the system. This hardware design applies bus supply power method to reduce system power consumption. In addition, the decoupling network consists of magnetic beads and has the capacity to store electricity. The USB is placed between the bus and FT245R, as shown in Figure 8. The FT245R current is 15 mA in a normal working environment; this current is lower than that in suspend mode.

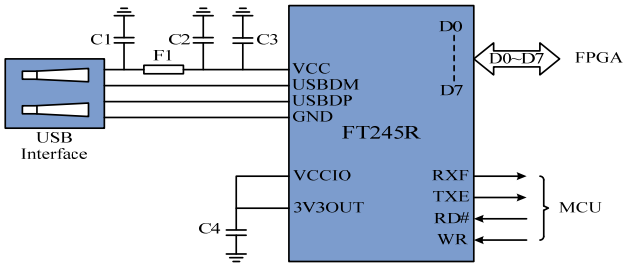

Figure 8. USB drive circuit

5. Testing Through Experimentation

The assembled testing system is illustrated in Figure 9. An ICP sensor is installed in the center of the mechanical shell, and the sensitive surface is located at the same level as the up-surface of the shell. A protective cover is situated at the periphery of the up-surface; this cover is connected to the screw thread, and the control panel is under the cover. This control panel mainly consists of a power switch, charging interface, USB interface, and state indicators. The switch is turned on prior to testing. Then, the testing system reloads the working parameters automatically. In the process, this system enters the triggering state. If the working parameters must be amended, then the system can connect a computer through the USB interface and can program parameters using specific software. Once the program is completed, the working parameters of the system can be refreshed and stored internally in E2PROM.

Figure 9. Image of the testing system

Figure 10. Image of a certain bomb during actual testing

Figure 10 shows the image of a static explosive experiment involving a certain bomb. The measured height of the wooden support under which a steel plate lies is 1.5 m. The projection of the central axis of the bomb is selected as the explosion center. The testing system applies this center as the center of a circle that radiates outward in three directions. Four testing dots are laid out in each direction as the set radii (distance between the testing dot and the explosion center) at 5, 7, 10, and 15 m. Figure 11 indicates the actual test data of a certain dot in direction 1. The result suggests that the peak shockwave overpressure generally conforms to the principles of monotone reduction because the testing dots are far from the explosion center. This finding also reflects the transmission characteristics of the explosive shockwave.

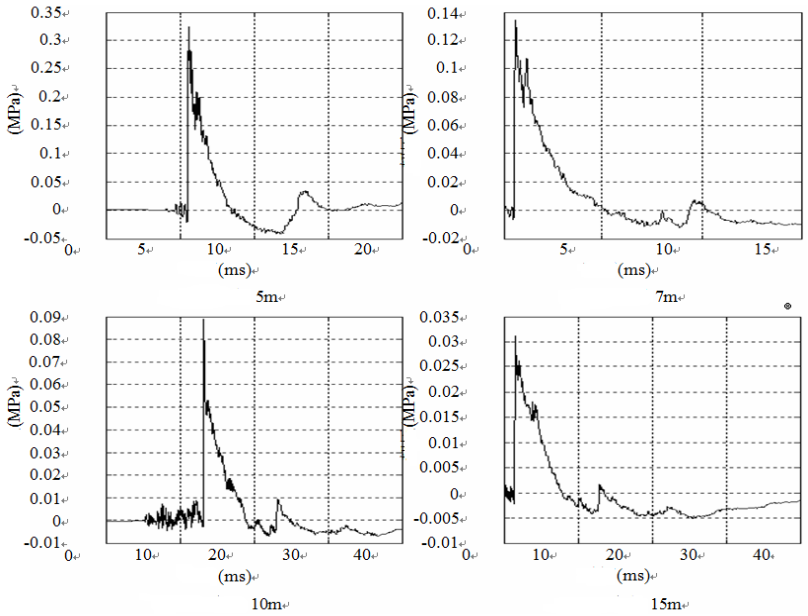

Figure 11. Actual testing curve

6. Conclusion

This study proposes a dynamic compensator design method based on the PSO algorithm. Output and input are obtained through sensor calibration and are maximized to produce an optimized dynamic compensator. The effect of modeling errors on the dynamic compensation of the sensor is avoided in the absence of dynamic modeling throughout the process. The distributed algorithm effectively amends the dynamic errors in sensors at high speed and online. The experimental result indicates that a high-speed parallel dynamic compensator can amend dynamic errors of sensors accurately and in real time.

References

[1] Liu Q, Cao GH. The Modeling Reference and the Dynamic Compensated Algorithm of the Errors Whitening Sensor. *Control Theory and Application*. 2009; 26(3): 256-260.
[2] Tian WJ, Liu JC. *A New Optimization Algorithm for Dynamic Compensation of Sensors*. Second International Conference on Computer Modeling and Simulation. 2010; 1: 1707-1710.
[3] Wu J, Zhang ZJ. *Real-time Correction for Sensor's Dynamic Error Based on DSP*. IEEE International Instrumentation and Measurement Technology Conference. 2011; 1: 633-638.
[4] Wang F, Lv FZ. Application of Nonlinear Adaptive Filter in the Signal Processing of Magnetostictive Guided Wave Transducer. *Chinese Journal of Sensors and actuators*. 2010; 23(11): 1594-1598.
[5] Chen S. Digital IIR filter design using particle swarm optimization. *Int J Modelling Identification and control*. 2010; 9(7): 327-335.
[6] Wu XJ, Zhang D. New measurement method of roundness error based on particle swarm optimization algorithms. *Chinese Jouranl of Sensors and actuators*. 2007; 20(4): 832-834.
[7] Zhong YQ, Zhao L. Design and implementation of receiver front-end filter in wireless sensor networks. *Chinese Journal of Sensors and actuators*. 2009; 22(7): 1034-1039.
[8] Sascha E, Alfred L. Dynamic Uncertainty for Compensated Second-Order Systems. *Sensors.* 2010; 10(8): 7621-7631.
[9] Fan BS, Tan GZ, Fan SS. Comparison of Three Different 2-D Space Vector PWM Algorithms and Their FPGA Implementations. *Journal of Power Technologies.* 2014; 94(3): 176-189.
[10] Sutikno T. FPGA for robotic applications: From android/humanoid robots to artificial men. *TELKOMNIKA (Telecommunication, Computing, Electronics and Control).* 2011; 9(3): 401-402.
[11] Harikrishna D. Dynamic stability enhancement of power systems using neural-network controlled static-compensator. *TELKOMNIKA (Telecommunication, Computing, Electronics and Control)*. 2013; 10(1): 9-12.